

See discussions, stats, and author profiles for this publication at: <https://www.researchgate.net/publication/26295004>

# Generation of correlated photons in nanoscale silicon waveguides

Article in *Optics Express* · January 2007

DOI: 10.1364/OE.14.012388 · Source: PubMed

CITATIONS

375

READS

390

8 authors, including:



**Jay E Sharping**

University of California, Merced

56 PUBLICATIONS 4,155 CITATIONS

[SEE PROFILE](#)



**Kim Fook Lee**

Northwestern University

89 PUBLICATIONS 1,324 CITATIONS

[SEE PROFILE](#)



**Alexander Gaeta**

Columbia University

746 PUBLICATIONS 33,533 CITATIONS

[SEE PROFILE](#)



**Prem Kumar**

Northwestern University

526 PUBLICATIONS 11,697 CITATIONS

[SEE PROFILE](#)

# Generation of correlated photons in nanoscale silicon waveguides

Jay E. Sharping,<sup>3</sup> Kim Fook Lee,<sup>1</sup> Mark A. Foster,<sup>3</sup> Amy C. Turner,<sup>2</sup> Bradley S. Schmidt,<sup>2</sup> Michal Lipson,<sup>2</sup> Alexander L. Gaeta,<sup>3</sup> and Prem Kumar<sup>1</sup>

<sup>1</sup>Center for Photonic Communication and Computing, Northwestern University, Evanston, IL 60208

<sup>2</sup>School of Electrical and Computer Engineering, Cornell University, Ithaca, NY 14853

<sup>3</sup>School of Applied and Engineering Physics, Cornell University, Ithaca, NY 14853

[jsharping@ucmerced.edu](mailto:jsharping@ucmerced.edu)

**Abstract:** We experimentally study the generation of correlated pairs of photons through four-wave mixing (FWM) in embedded silicon waveguides. The waveguides, which are designed to exhibit anomalous group-velocity dispersion at wavelengths near 1555 nm, allow phase matched FWM and thus efficient pair-wise generation of non-degenerate signal and idler photons. Photon counting measurements yield a coincidence-to-accidental ratio (CAR) of around 25 for a signal (idler) photon production rate of about 0.05 per pulse. We characterize the variation in CAR as a function of pump power and pump-to-sideband wavelength detuning. These measurements represent a first step towards the development of tools for quantum information processing which are based on CMOS-compatible, silicon-on-insulator technology.

©2006 Optical Society of America

**OCIS codes:** (230.7380) Optical devices, Waveguides, channeled; (190.4380) Nonlinear optics, four-wave mixing; (270.4180) Quantum optics, Multiphoton processes

---

## References and links

1. M. A. Nielsen and I. L. Chuang, *Quantum Computation and Quantum Information* (Cambridge University Press, Cambridge, MA, 2000).
2. D. Bouwmeester, A. Ekert, and A. Zeilinger, eds., *The Physics of Quantum Information* (Springer-Verlag, Berlin, 2000).
3. A. C. Turner, C. Manolatou, B. S. Schmidt, M. Lipson, M. A. Foster, J. E. Sharping, and A. L. Gaeta, "Tailored anomalous-group velocity dispersion in silicon channel waveguides," *Opt. Express* **14**, 4357-4362 (2006).
4. D. Dimitropoulos, V. Raghunathan, R. Claps, and B. Jalali, "Phase-matching and nonlinear optical processes in silicon waveguides," *Opt. Express* **12**, 149-160 (2004).
5. L. Yin, Q. Lin, and G. P. Agrawal, "Dispersion tailoring and soliton propagation in silicon waveguides," *Opt. Lett.* **31**, 1295-1297 (2006).
6. M. A. Foster, A. C. Turner, J. E. Sharping, B. S. Schmidt, M. Lipson, and A. L. Gaeta, "Broad-band optical parametric gain on a silicon photonic chip," *Nature* **441**, 960-963 (2006).
7. Q. Lin and G. P. Agrawal, "Silicon waveguides for creating quantum-correlated photon pairs," *Opt. Lett.* **31**, 3140-3142 (2006).
8. M. Fiorentino, P. L. Voss, J. E. Sharping, and P. Kumar, "All-fiber photon-pair source for quantum communications," *IEEE Photon. Technol. Lett.* **14**, 983-985 (2002).
9. J. Sharping, J. Chen, X. Li, P. Kumar, and R. Windeler, "Quantum-correlated twin photons from microstructure fiber," *Opt. Express* **12**, 3086-3094 (2004).
10. J. Fan, A. Migdall, and L. J. Wang, "Efficient generation of correlated photon pairs in a microstructure fiber," *Opt. Lett.* **30**, 3368-3370 (2005).
11. J. Chen, X. Li, and P. Kumar, "Two-photon-state generation via four-wave mixing in optical fibers," *Phys. Rev. A* **72**, 033801 (2005).
12. O. Alibart, J. Fulconis, G. K. L. Wong, S. G. Murdoch, W. J. Wadsworth, and J. G. Rarity, "Photon pair generation using four-wave mixing in a microstructured fibre: theory versus experiment," *New J. Phys.* **8**, 67-86 (2006).
13. Q. Lin, F. Yaman, and G. P. Agrawal, "Photon-pair generation by four-wave mixing in optical fibers," *Opt. Lett.* **31**, 1286-1288 (2006).

14. X. Li, P. L. Voss, J. E. Sharping, and P. Kumar, "Optical-fiber source of polarization-entangled photons in the 1550 nm telecom band," *Phys. Rev. Lett.* **94**, 053601 (2005).
15. H. Takesue and K. Inoue, "Generation of 1.5- $\mu$ m band time-bin entanglement using spontaneous fiber four-wave mixing and planar light-wave circuit interferometers," *Phys. Rev. A* **72**, 041804(R) (2005).
16. X. Li, J. Chen, P. Voss, J. Sharping, and P. Kumar, "All-fiber photon-pair source for quantum communications: Improved generation of correlated photons," *Opt. Express* **12**, 3737-3744 (2004).
17. M. Hass, "Raman spectra of vitreous silica, germania, and sodium silicate glass," *J. Phys. Chem. Solids* **31**, 415-422 (1970).
18. D. J. Dougherty, F. X. Kaertner, H. A. Haus, and E. P. Ippen, "Measurement of the Raman gain spectrum of optical fibers," *Opt. Lett.* **20**, 31-33 (1995).
19. J. H. Parker, D. W. Feldman, M. Ashkin, "Raman scattering by silicon and germanium," *Phys. Rev.* **155**, 712-714 (1967).
20. D. Dimitropoulos, R. Jhaveri, R. Claps, J. C. S. Woo, and B. Jalali, "Lifetime of photogenerated carriers in silicon-on-insulator rib waveguides," *App. Phys. Lett.* **86**, 071115 (2005).
21. V. R. Almeida, C. A. Barrios, R. R. Panepucci, M. Lipson, M. A. Foster, D. G. Ouzounov, and A. L. Gaeta, "All-optical switching on a silicon chip," *Opt. Lett.* **29**, 2867-2869 (2004).
22. Q. Xu, V. Almeida, and M. Lipson, "Time-resolved study of Raman gain in highly confined silicon-on-insulator waveguides," *Opt. Express* **12**, 4437-4442 (2004).
23. M. Dinu, F. Quochi, and H. Garcia, "Third-order nonlinearities in silicon at telecom wavelengths," *Appl. Phys. Lett.* **82**, 2954-2956 (2003).
24. P. L. Voss, K. G. Koprulu, S.-K. Choi, S. Dugan, and P. Kumar, "14 MHz rate photon counting with room temperature InGaAs/InP avalanche photodiodes," *J. Mod. Opt.* **15**, 1369-1379 (2004).
25. K. F. Lee, J. Chen, C. Liang, X. Li, P. L. Voss, and P. Kumar, "Generation of high-purity telecom-band entangled photon pairs in dispersion-shifted fiber," *Opt. Lett.* **31**, 1905-1907 (2006).
26. G. N. Gol'tsman, O. Okunev, G. Chulkova, A. Lipatov, A. Semenov, K. Smirnov, B. Voronov, A. Dzardanov, C. Williams, and R. Sobolewski, "Picosecond superconducting single-photon optical detector," *Appl. Phys. Lett.* **79**, 705-707 (2001).
27. C. Liang, K. F. Lee, M. Medic, P. Kumar, and S. W. Nam, "Characterization of fiber-generated entangled photon pairs with superconducting single-photon detectors," submitted to *Opt. Express*.

## 1. Introduction

In recent years, scientists have begun to find situations where quantum-mechanically rich systems provide unique solutions to modern technological problems. Quantum information processing (QIP) forms one arena for promising applications of such systems [1, 2]. Information storage, data transmission, and certain logic operations and algorithms can benefit when implemented using quantum-mechanical approaches. Quantum-optical systems are particularly important where the quanta of light are photons whose quantum-mechanical state can be described, for example, in terms of physical attributes such as polarization, energy, and/or direction of propagation [2].

The success of "classical" information processing owes much to advances in semiconductor technology such as the ability to make devices in silicon in an integrated and scaleable manner. As an example, complementary metal-oxide semiconductor (CMOS) fabrication technology has allowed for fast, low-power implementation of densely-packed transistors. In the same vein, the future successful implementation of quantum information technology depends heavily on finding a similar platform for low-power, scaleable operation of QIP devices.

In this paper, we describe a first step towards practical QIP devices based on silicon optical waveguide technology. We report on a source of correlated pairs of photons that are generated within a silicon waveguide. Fabricated using CMOS-compatible technology, the nanoscale waveguide dimensions are tailored [3-5] to allow for efficient four-wave mixing [6], resulting in the simultaneous creation of pairs of photons, called signal and idler, whose energies are well defined with respect to one another. Quantum information processing using phase-matched FWM in Si waveguides was suggested in [6] and an explicit model for creating quantum-correlated photon pairs has been recently presented [7]. Similar four-wave mixing (FWM) in optical fibers has been used to generate pairs of photons [8-13] exhibiting polarization and time-bin entanglement [14, 15], which are particularly useful for quantum communications applications. The work described here is the first demonstration of the generation of quantum-correlated photons in an integrated silicon system. It also represents a

first step in the creation of a scaleable platform for quantum optical technology that is “backward compatible” with the existing silicon-based information processing infrastructure.

In the previous work on generating correlated and entangled photons using FWM in optical fibers [8-16] spontaneous Raman scattering (SRS) is the principal fundamental source of noise [16]. Uncorrelated photons are produced when pump photons couple with inhomogeneously-broadened vibrational Raman modes of the silica molecules [17, 18]. As such, we are motivated to work with silicon because we expect the quantum noise due to SRS in silicon waveguides [19-22] to behave differently than in glass because of the crystalline nature of the silicon material, which leads to significantly lesser broadening of the Raman vibrational modes.

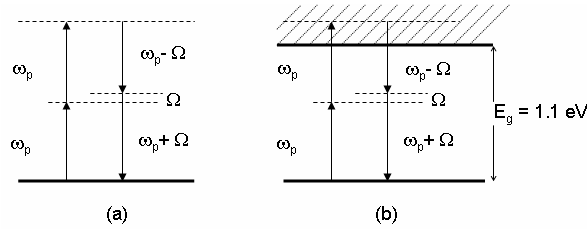


Fig. 1. Description of the FWM process in (a) optical fibers, and (b) silicon waveguides.

The FWM process arises from the  $\chi^{(3)}$  nonlinearity of the optical fiber, as depicted in Fig. 1(a). Two pump photons of the same angular frequency  $\omega_p$  are destroyed in order to create two other photons which are detuned in frequency from that of the pump by  $\pm\Omega$ . Energy is conserved in this process and, for optical fibers, higher energy states are far detuned from the virtual levels shown in the diagram. Pump photons, which are confined to the core of the fiber, induce an electronic polarization in the material which then couples with photons of other optical frequencies. The coupling coefficient,  $\gamma$ , in standard dispersion-shifted fibers is roughly  $3 \text{ (W}\cdot\text{km)}^{-1}$ , but for microstructure fibers  $\gamma$  can be greater than  $100 \text{ (W}\cdot\text{km)}^{-1}$ . Efficient coupling also depends upon phase matching of the propagation constants of the photons involved and is often achieved by operating in a wavelength region where the group-velocity dispersion (GVD) is anomalous and small in magnitude. In waveguides (including fibers), the GVD depends on the dispersive properties of the material and on the design of the waveguide.

For nanoscale waveguides fabricated in silicon the relatively large susceptibility leads to  $\gamma \approx 100,000 \text{ (W}\cdot\text{km)}^{-1}$ , which indicates that significant nonlinear effects can be observed in device lengths of 1 cm or less [23]. The strong mode-field confinement and large refractive-index contrast leads to dispersive properties that are extremely sensitive to the waveguide dimensions, so the waveguide must be carefully designed to obtain the anomalous dispersion required for phase matching the FWM process [3-5]. One must also consider the presence of excited energy levels, as depicted in Fig. 1(b). Individual photons with wavelengths of  $1.5 \mu\text{m}$  do not carry sufficient energy to span the bandgap, but nonlinear, multi-photon absorption is possible. In addition, carriers excited into the valence band can be further excited to a continuum of higher energy levels through excited state absorption which represents a loss process for the FWM photons.

## 2. Experiment

The experimental setup is illustrated schematically in Fig. 2. Light from a femtosecond fiber laser (IMRA, FemtoLite) is filtered at 1556 nm through a 1 nm-bandwidth tunable filter, and then amplified in an erbium-doped fiber amplifier (EDFA). The amplified spontaneous emission from the EDFA is further suppressed by using three cascaded wavelength-division multiplexing (WDM) filters with a full-width at half maximum (FWHM) of about 1 nm to obtain 5-ps pump pulses at 1556 nm with a repetition rate of 50 MHz. This filtering provides

more than 140 dB of side-band suppression in the spectral region where photon counting is performed on the FWM-generated signal/idler photons. Although the filters do not select signal/idler photons from the peaks of the phase-matching curve of the waveguide [6], we use this source and filter system because it is well characterized and has been used in other experiments to make similar measurements [27]. The pump pulses are launched into a 9.11-mm long silicon-on-insulator waveguide with transverse dimensions of 600 nm x 300 nm. Light is coupled into the waveguide using a lensed fiber and an inverse taper as described in Almeida, *et al.* [21]. The electric-field polarization, adjusted using a fiber polarization controller, is made parallel with the long dimension of the waveguide, corresponding to the so-called TE-like mode. The linear loss through the waveguide is  $\sim -1.1$  dB [6]. The output is collected using a short focal-length aspheric lens, passed through a polarizer, and then coupled into a single-mode fiber using another aspheric lens. The net collection efficiency is estimated to be about 8% which is comprised of 40% output coupling efficiency from the waveguide inverse taper and collection lens and 20% coupling efficiency from free space into the single-mode fiber. The single-mode fiber leads to a set of WDM filters which are used to spectrally separate the correlated pairs and to suppress leakage of the pump photons through to the photon counters. The pass-band for the detected signal and idler photons is super-Gaussian with a FWHM of 1 nm and a throughput transmissivity of 0.8 in each band.

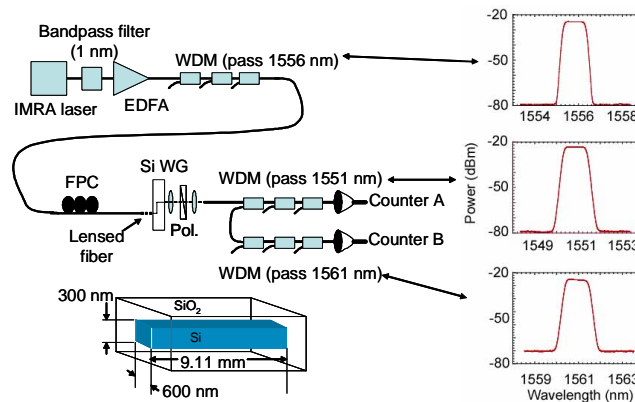


Fig. 2. Schematic of the setup used to observe correlated photon scattering in silicon waveguides. Shown on the right are the pass bands for each set of WDM filters. A schematic of the Si waveguide buried in SiO<sub>2</sub> is shown as an inset.

Photon counting is performed with InGaAs avalanche photodiodes operated in gated, Geiger mode [8, 24]. The gating is done at a rate down counted from the repetition rate of the laser, such that the detectors operate at 781 kHz. The quantum efficiency of these detectors is about 20%, with a dark-count probability of  $2 \times 10^{-3}$  per gate pulse. The total detection efficiency is thus 1.3% after the 8% photon-pair collection efficiency and the 80% WDM-filter transmissivity are taken into account. The counters are interrogated by a computer to obtain the signal counts and the idler counts as a function of time. Coincidence counts are derived from such data by directly comparing the two data strings, and accidental counts are derived by comparing the two data strings where one string is shifted in time by one gate period. For each set of data, dark counts are also recorded at the beginning and end of the experiment.

The largest average power measured after the collection lens is 176  $\mu$ W, which corresponds to 700 mW peak power in the pump pulses. The peak power within the waveguide, after accounting for output coupling losses, is then 1.8 W. As discussed below, the best ratio for coincidence to accidental counts (about 25) is achieved at about 240 mW of peak pump power.

Before making the photon-counting measurements, we verify that the system is aligned optimally, and configured in a spectral region where phase-matched FWM is possible. This is achieved by observing macroscopic mixing between a strong pump and an injected probe field at the signal wavelength. When the system is properly aligned, the probe mixes with the pump to create an idler in the conjugate sideband as observed on an optical spectrum analyzer. The alignment, once achieved, is stable for several hours, which is critical for obtaining high quality photon-counting data with good signal-to-noise ratio.

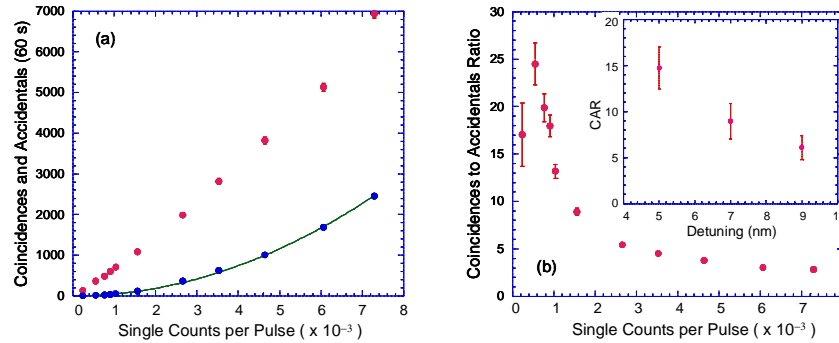


Fig. 3. Results from coincidence-counting measurements. (a) Plots of total coincidences (red) and accidental coincidences (blue) versus single counts per pulse obtained as the pump power is increased. The latter plot is in excellent agreement with the expected quadratic dependence (solid line). (b) Plot of the ratio of coincidences to accidental coincidences (CAR) versus single counts per pulse. Inset in (b) is a plot of the CAR as a function of the detuning of the signal and idler filters from the pump wavelength.

Figure 3 presents the experimental photon-counting data showing how the coincidence-counting behavior changes as the pump power is increased in both the coincident time windows (coincidences) and the adjacent time windows (accidentals), where the x-axis is expressed as the single counts per pulse (geometric average of the single counts in the signal and idler channels) and the contributions of the measured dark counts have been subtracted from the data. As shown in Fig. 3(a), at low single-count rates (see below), both the coincidence rate and the accidentals rate grow as the power increases, but the coincidence rate shows a noticeably larger increase. This approximates the ideal case in which the coincidences are an increasing function of power and the accidentals are zero, which corresponds to the case in which photon pairs are generated only by FWM. We plot the coincidences-to-accidentals ratio (CAR), which is a measure often used to evaluate the degree of correlations in the generated light [10-12,15]. This is presented in Fig. 3(b) wherein we see that there is a rapid increase in the CAR as the single-count rate increases until it reaches about  $6 \times 10^{-4}$ , which corresponds to a photon-pair generation rate of  $0.0006/0.013 = 0.05$  in the waveguide. For larger single-count rates the CAR decreases. Interestingly, similar behavior is observed in correlated-photon sources based on glass fibers [25]. The behavior at low count rates, we presently believe, is caused by the increasing contribution of the detector dark counts, which cannot be reliably subtracted when the single-count rate becomes too low [15]. Our recent measurements with superconducting single-photon detectors [26] corroborate this hypothesis [27]. The decrease in CAR for single-count rates greater than 0.001 is attributed to increasing multi-photon scattering probability.

Measurements similar to those in Fig. 3 are also obtained when the polarizer in the free space path between the waveguide and the collection fiber is left out (see Fig. 2). In this case the measured CAR is slightly lower (about 17), suggesting that uncorrelated noise photons polarized orthogonally with respect to the pump are also produced. Since the FWM process is only phase matched for co-polarized pump, signal, and idler photons, the presence of noise in

the other polarization component suggests there is another mechanism, such as SRS, that generates accidental counts.

As sketched in Fig. 1(b), the presence of excited energy levels plays an important role in light interactions within silicon waveguides. There have been several relevant publications that call attention to the dynamics of the generated carriers (electrons and holes) in silicon waveguides [20-22]. Dimitropoulos, *et al.* [20] address this point head on by simulating the carrier lifetimes in sub-micron waveguide structures. In essence, the bulk recombination lifetimes, which are about 2  $\mu$ s for electrons and 10  $\mu$ s for holes, are modified by diffusion into and out of the optically excited portion of the waveguide. As the transverse dimensions of the waveguide are made smaller, the free-carrier lifetimes become shorter. The simulations in Ref. [20] for a 600-by-300 nm rib waveguide imply lifetimes on the order of 700-900 ps. Data presented by Almeida, *et al.* [21] describe more closely the waveguides that we are using. This paper introduces an optical switch formed from a silicon ring microresonator, where the performance implies a free-carrier recombination lifetime of about 450 ps. According to the analysis in Ref. [21], the free-carrier lifetime can be made shorter by further manipulation of the sidewall structure. Another very interesting switching paper is that by Xu, *et al.* [22], wherein they describe a switch based on free-carrier dispersion and Raman gain. Through the combined effects of Raman amplification and free-carrier dispersion, they see switching with a high extinction ratio (>20 dB). According to the results in Ref. [22], free-carrier dispersion is worth investigating as a source of additional noise photons.

In order to gain further understanding into the source of the observed accidentals, we studied the CAR for different values of the pump to detection-filter separation. For each filter separation, the CAR as a function of single counts per pulse was measured and the peak CAR are plotted in the inset of Fig. 3(b) wherein one observes that the quality of the correlations decreases as the filters are tuned further from the pump. The CAR for 5-nm detuning in this case is not as high as that reported in Fig. 3(a) because the tunable filters with which these measurements are taken have different transmission characteristics. The CAR versus detuning data suggest that the source of noise photons does not arise from carrier dynamics or free-carrier dispersion, as it is unlikely that these mechanisms would have bandwidths exceeding a few hundred GHz. For noise of this sort one would expect the CAR to increase as the filter separation increases, which is not observed in our measurements. The source of accidentals in this system is still under investigation.

### 3. Conclusion

We have reported a significant first step towards integrated quantum optical technology for information processing. Despite our experimental limitations in the collection and detection of correlated photons, the pair-generation effect could still be observed in a chip-scale silicon platform. The generation of correlated photons within a CMOS-compatible silicon waveguide, combined with the ability to fabricate complex structures such as couplers, filters, detectors, and other optoelectronic components on the same silicon platform, represents a golden opportunity for the development of scaleable quantum information processing devices.

### Acknowledgments

At Cornell this work was supported by the NSF through the Center for Nanoscale Systems under award number EEC-0117770. A.C.T. also acknowledges support under a NSF Graduate Research Fellowship. M.A.F., J.E.S., and A.L.G. also acknowledge support under the DARPA Slow-Light Program. This work was performed in part at the Cornell NanoScale Facility, a member of the National Nanotechnology Infrastructure Network, which is supported by the NSF (Grant ECS-0335765). The work at Northwestern was supported by the NSF (Grant No. EMT-0523975) and by DARPA and the AFOSR through an HP subcontract under AFOSR contract No. FA9550-05-C-0017.